

Fig. 3.4. The nature of finite-temperature QCD phase structure as a function of quark masses m_q and m_s .

plasma. However, experimental searches for quarks have not succeeded [186]. The experimental limits which were set suggest that confinement is a fundamental physical property. This being the case, we are of the opinion that, in the physical world, the transformation from the confined to the deconfined phase is a discontinuous phase transition, most likely of first order. For this reason, we placed the physical quark-mass point within the region of first-order phase transition in Fig. 3.4. This topical area is undergoing a rapid evolution.

4 Statistical properties of hadronic matter

4.1 Equidistribution of energy

The physical tools required to describe in further detail the properties of hot hadronic matter are much like the usual ones of statistical physics, which we briefly introduce and review. A more detailed analysis will follow.

Consider a large number N of identical coupled systems, distinguishable, e.g., by their energies E_i . To simplify the matter, we assume that

the energies E_i can assume only discrete values, and that there are K different ‘macro’ states such that $K \ll N$. Some of the energies of the macro states will be equal, i.e., most are occupied more often than once, and in general n_i times. The total energy,

$$E^{(N)} = \sum_{i=1}^K n_i E_i, \quad (4.1)$$

is conserved. Further below, we will introduce also conservation of a discrete quantum number, e.g., the baryon number. We note another subsidiary condition arising from the definitions:

$$\sum_i^K n_i = N. \quad (4.2)$$

Without an additional quantum number, systems with the same energy E_i are equivalent, i.e., in the language of quantum statistics, indistinguishable.

The distribution $\mathbf{n} = \{n_i\}$ having the same energy E_i can be achieved in many different ways. To find how many, consider the relation

$$\begin{aligned} K^N &= (x_1 + x_2 + \cdots + \cdots x_K)^N \Big|_{x_i=1} \\ &= \sum_{\mathbf{n}} \frac{N!}{n_1! n_2! \cdots n_K!} x_1^{n_1} x_2^{n_2} \cdots x_K^{n_K} \Big|_{x_i=1}. \end{aligned} \quad (4.3)$$

The normalized coefficients,

$$\boxed{W(\mathbf{n}) = \frac{K^{-N} N!}{\prod_{i=1}^K n_i!}}, \quad (4.4)$$

are the relative probabilities of realizing each state in the ensemble \mathbf{n} , with n_i equivalent elements. The practical way to find the most probable distribution $\bar{\mathbf{n}}$ is to seek the maximum of $\ln W$, Eq. (4.4), subject to the constraints Eqs. (4.1) and (4.2),

$$A(n_1, n_2, \dots, n_K) = \ln W(\mathbf{n}) - a \sum_i n_i - \beta \sum_i n_i E_i, \quad (4.5)$$

characterized by two Lagrange multipliers a and β . We differentiate Eq. (4.5) with respect to the n_i :

$$\frac{\partial}{\partial n_i} [-\ln(n_i!) - n_i a - \beta n_i E_i] \Big|_{\bar{\mathbf{n}}_m} = 0. \quad (4.6)$$

Insofar as all $\bar{n}_i \gg 1$, we can use the relation

$$\frac{d}{dk} [\ln(k!)] \approx \frac{\ln(k!) - \ln[(k-1)!]}{(k) - (k-1)} = \ln k. \quad (4.7)$$

One obtains for the maximum of the distribution Eq. (4.4), i.e., for the statistically most probable distribution $\bar{\mathbf{n}} = \{\bar{n}_i\}$, the well-known exponential

$$\boxed{\bar{n}_i = \gamma e^{-\beta E_i}}, \quad (4.8)$$

where the inverse of the slope parameter β is identified below as the temperature:

$$\boxed{T \equiv 1/\beta}. \quad (4.9)$$

The supplementary condition Eq. (4.2), given the set $\bar{\mathbf{n}}$, now reads

$$\sum_i \bar{n}_i = \gamma \sum_{i=1}^K e^{-\beta E_i} = N. \quad (4.10)$$

The quantity γ ,

$$\boxed{\gamma \equiv e^{-a}}, \quad (4.11)$$

as seen in Eq. (4.10), controls the total number of members of the ensemble N . It is the chemical fugacity introduced in section 1.1. We will meet both statistical parameters T and γ many times again in this book.

Employing Eq. (4.8), we find for the energy $E^{(N)}$, Eq. (4.1),

$$E^{(N)} = \sum_i \bar{n}_i E_i = \gamma \sum_i E_i e^{-\beta E_i}. \quad (4.12)$$

On dividing $E^{(N)}$ by N , we obtain the average energy of each member of the ensemble:

$$\boxed{\frac{E^{(N)}}{N} \equiv \overline{E^{(N)}} = \frac{\gamma \sum_i E_i e^{-\beta E_i}}{\gamma \sum_i e^{-\beta E_i}} \equiv -\frac{d}{d\beta} \ln Z}. \quad (4.13)$$

We introduced here the *canonical partition function* Z :

$$\boxed{Z = \sum_i \gamma e^{-\beta E_i}}. \quad (4.14)$$

Unlike the microscopic (micro-canonical) approach in which the energy for each member of the ensemble is fixed, in the statistical ‘canonical’ approach, one studies the most likely distribution of energy and other physical properties among members of the ensemble. These properties are controlled solely by the statistical parameters β and γ which are the Lagrange multipliers related to the conservation of energy, and the number of members of the ensemble.

4.2 The grand-canonical ensemble

We will now relax the assumption that only energy is equipartioned as it is exchanged between macro systems. In the *grand-canonical* approach, we seek the most probable statistical distribution allowing for the flow of a discrete quantum number between the individual members of the statistical ensemble. In passing, we also show how the mathematical framework of the grand-canonical approach offers a convenient path to the evaluation of the canonical ensemble quantities, when discrete conservation laws apply.

We proceed in every detail as before, but need to characterize each macro state by an additional discrete number, and we need to introduce a further subsidiary condition to assure that this (baryon) number is conserved:

$$\sum_{i=1}^N n_i^b b_i = b^{(N)} \equiv N \bar{b}_i. \quad (4.15)$$

Here, \bar{b}_i is the average number of baryons in each ensemble member considered. The condition Eq. (4.15) introduces a further constraining Lagrange parameter into Eq. (4.6), which we write in the form $-\ln \lambda$. In this way the generalization of Eq. (4.6) is

$$\left. \frac{\partial}{\partial n_i^b} \left[-\ln(n_i^b!) - n_i^b a - \beta n_i^b E_i + \ln \lambda n_i^b b_i \right] \right|_{\bar{n}_m} = 0. \quad (4.16)$$

Proceeding as in section 4.1, we obtain the most probable distribution of \bar{n}_i as

$$\bar{n}_i^b = \gamma \lambda^{b_i} e^{-\beta E_i}, \quad (4.17)$$

where the number of particles is controlled by the fugacity factor λ and the factor $\gamma = e^{-a}$, see Eq. (4.11). It is common practice to introduce the chemical potential μ :

$$\boxed{\mu \equiv T \ln \lambda, \quad \lambda = e^{\beta \mu} = e^{\mu/T}.} \quad (4.18)$$

The chemical potentials shown have physical meaning, and determine the energy required to add/remove a particle at fixed pressure, energy, and entropy. Following the method that led us to Eq. (4.13), we obtain

$$\boxed{\overline{E}_{(N)} = \gamma \frac{\sum_{i;b} E_i \lambda^{b_i} e^{-\beta E_i}}{\gamma \sum_{i;b} \lambda^{b_i} e^{-\beta E_i}} \equiv -\frac{d}{d\beta} \ln \mathcal{Z}.} \quad (4.19)$$

We have introduced the grand-canonical partition function \mathcal{Z} :

$$\mathcal{Z}(V, \beta, \lambda) = \gamma \sum_{i;b} \lambda^{b_i} e^{-\beta E_i}. \quad (4.20)$$

\mathcal{Z} is in fact also a ‘generating’ function for the canonical partition function Z_b ,

$$Z_b(V, \beta) = \frac{1}{2\pi i} \oint db \frac{1}{\lambda^{b+1}} \mathcal{Z}(\beta, \lambda), \quad (4.21)$$

where $Z_b(V, \beta)$ describes a system with a fixed baryon number b . The path of integration in Eq. (4.21) leads around the singularity at $\lambda = 0$; it is often chosen to be the unit circle.

We can also evaluate the average value of b for the grand-canonical partition function:

$$\begin{aligned} \bar{b} &= \frac{\sum_{i;b} b_i \lambda^{b_i} e^{-\beta E_i}}{\sum_{i;b} \lambda^{b_i} e^{-\beta E_i}}, \\ &= \lambda \frac{d}{d\lambda} \left(\ln \sum_{i;b} \gamma \lambda^{b_i} e^{-\beta E_i} \right) \equiv \lambda \frac{d}{d\lambda} \ln \mathcal{Z}(\beta, \lambda). \end{aligned} \quad (4.22)$$

4.3 Independent quantum (quasi)particles

Elementary quantum physics allows a simple evaluation of the grand-canonical partition function. The discrete energies E_i of the physical systems in the statistical ensemble we introduced above are now to be understood as eigenenergies with eigenstate $|i\rangle$ of a quantum Hamiltonian \hat{H} :

$$\hat{H}|i\rangle = E_i|i\rangle. \quad (4.23)$$

Since the (conserved-baryon-number) operator \hat{b} commutes with the Hamiltonian, $[\hat{b}, \hat{H}] = 0$, the eigenstates can furthermore be characterized by their baryon number (and strangeness, and other discrete quantum numbers that are constants of motion, but we restrict the present discussion to the baryon number only). We have

$$\hat{b}|i, b\rangle = b|i, b\rangle. \quad (4.24)$$

The grand-canonical partition function, Eq. (4.20), can be written as

$$\begin{aligned} \mathcal{Z} &\equiv \sum_{i,b} \langle i, b | \gamma e^{-\beta(\hat{H} - \mu \hat{b})} | i, b \rangle = \text{Tr} \gamma e^{-\beta(\hat{H} - \mu \hat{b})}, \\ &\equiv \sum_n \langle n | e^{-\beta(\hat{H} - \mu \hat{b} - \beta^{-1} \ln \gamma)} | n \rangle. \end{aligned} \quad (4.25)$$

The great usefulness of this relation is that the trace of a quantum operator is representation-independent; that is, any complete set of microscopic basis states $|n\rangle$ may be used to find the (quantum) canonical or grand-canonical partition function. This allows us to obtain the physical properties of quantum gases in the, often useful, approximation that they consist of practically independent (quasi)particles, and, eventually, to incorporate any remaining interactions by means of a perturbative expansion.

The reference to quasi-particles is made since, e.g., in a medium, masses of particle-like objects can be different from masses of ‘elementary’ particles. Generally there will be collective excitation modes characterized by a mass spectrum. In this respect, dense hadronic matter behaves like any dense-matter system. As long as there is a set of well-defined excitations, it really does not matter whether we are dealing with real particles or quasi-particles, when we compute the trace of the quantum partition function Eq. (4.25). Putting it differently, even though we compute the properties of a ‘free’-particle quantum gas, by choosing a suitable quasi-particle basis, we accommodate much of the effect of the strong interactions between particles.

The ‘single (quasi)particle’ occupation-number basis is the suitable one for the evaluation of the trace in Eq. (4.25). In this approach, each macro state $|n\rangle$ is characterized by the set of occupation numbers $\mathbf{n} = \{n_i\}$ of the single (quasi)particle states with baryon charge b_i of energy ε_i , and the state energy is given by $E_n = \sum_i n_i \varepsilon_i$. The sum over all possible states corresponds to a sum over all allowed sets \mathbf{n} : for fermions, each $n_i \in 0, 1$ and for bosons, $n_i \in 0, 1, 2, \dots, \infty$:

$$\begin{aligned} \mathcal{Z} &= \sum_{\mathbf{n}} e^{-\sum_{i=1}^{\infty} n_i \beta (\varepsilon_i - \mu b_i - \beta^{-1} \ln \gamma)}, \\ &= \sum_{\mathbf{n}} \prod_i e^{-n_i \beta (\varepsilon_i - \mu b_i - \beta^{-1} \ln \gamma)}. \end{aligned} \tag{4.26}$$

In this case the sum and product can be interchanged:

$$\sum_{\mathbf{n}} \prod_i e^{-n_i \beta (\varepsilon_i - \mu b_i - \beta^{-1} \ln \gamma)} = \prod_i \sum_{n_i=0,1,\dots} e^{-n_i \beta (\varepsilon_i - \mu b_i - \beta^{-1} \ln \gamma)}. \tag{4.27}$$

To show this equality, one considers whether all the terms on the left-hand side are included on the right-hand side, where the sum is not over all the sets of occupation numbers \mathbf{n} , but over all the allowed values of occupation numbers n_i . For fermions (F, Fermi–Dirac statistics) we can have only $n_i = 0, 1$, whereas for bosons (B, the Bose–Einstein statistics) $n_i = 0, 1, \dots, \infty$. The resulting sums are easily carried out analytically:

$$\ln \mathcal{Z}_{F/B} = \ln \prod_i \left(1 \pm \gamma e^{-\beta(\varepsilon_i - \mu b_i)} \right)^{\pm 1} = \pm \sum_i \ln(1 \pm \gamma \lambda_i^b e^{-\beta \varepsilon_i}). \tag{4.28}$$

The plus sign applies to F, and the minus sign to B; fermions have Pauli occupancy 0, γ , of each distinct single-particle state, and bosons have occupancy 0, $\gamma^1, 2\gamma^2, \dots, \infty$. The factor γ^n arises naturally since we have not tacitly set the occupancy of each single-particle level to unity as is commonly done when absolute chemical equilibrium is assumed.

For antiparticles, the eigenvalue of \hat{b} , in Eq. (4.28), is the negative of the particle value. Consequently, the fugacity $\lambda_{\bar{f}}$ for antiparticles \bar{f} is

$$\boxed{\lambda_{\bar{f}} = \lambda_f^{-1}.} \quad (4.29)$$

It is convenient to also introduce this change in sign into the definition of the chemical potential, see Eq. (4.18), and to introduce particle and antiparticle chemical potentials such that

$$\boxed{\mu_f = -\mu_{\bar{f}}.} \quad (4.30)$$

These relations, Eqs. (4.29) and (4.30), will often be implied in what follows in this book. The microscopic (quasi)particle energy is denoted by ε in Eq. (4.28). For a homogeneous space-time, it is determined in terms of the momentum \vec{p} in the usual manner:

$$\boxed{\varepsilon_i = \sqrt{m_i^2 + \vec{p}^2}.} \quad (4.31)$$

In order to make any practical evaluations of Eq. (4.28), we need to interpret the level sum \sum_i with some precision. If energy is the only controlling factor then we carry out this summation in terms of the single-particle level density $\sigma_1(\varepsilon, V)$:

$$\sum_i [\dots] = \int d\varepsilon \sigma_1(\varepsilon, V) [\dots]. \quad (4.32)$$

To obtain σ_1 , i.e., the number of levels in a box of (infinite) volume $V = L^3$ per unit of energy ε , we note that quantum mechanics does not allow a continuous range of \vec{p} in Eq. (4.31).

We consider a box L^3 with periodic boundary conditions and obtain the complete set of plane-wave states ψ having the required periodicity,

$$\psi \propto e^{i(\vec{p}_\alpha \cdot \vec{X})} = e^{i\vec{p}_\alpha(\vec{X} + \vec{n}L)}, \quad (4.33)$$

where $\vec{n} = (n_1, n_2, n_3)$ with $n = 0, \pm 1, \pm 2, \dots$. This fixes the allowed \vec{p}_α to

$$L\vec{p}_\alpha \cdot \vec{n} = 2\pi k, \quad k = 0, \pm 1, \pm 2, \dots \quad (4.34)$$

This can be satisfied only if

$$\vec{p}_\alpha = \frac{2\pi}{L}(k_1, k_2, k_3), \quad \text{with } k_i = 0, \pm 1, \pm 2, \dots \quad (4.35)$$

To sum over all single-particle states, we sum over all k_i . The number of permitted states equals the number of lattice points in the ‘inverse’ or ‘phase-space’ k -lattice. In the limit of large L ,

$$[\text{number of states in } d^3k] = \left(\frac{L}{2\pi}\right)^3 d^3p = \frac{V}{(2\pi)^3} d^3p. \quad (4.36)$$

Thus, we obtain the single-level density, Eq. (4.32):

$$\sum_i [\dots] = \int d\varepsilon \frac{V d^3p}{(2\pi)^3} \frac{d^3p}{d\varepsilon} [\dots]. \quad (4.37)$$

We keep in mind that, in general, the replacement of the discrete-level sum implies, in the limit of infinite volume of the system the phase-space integral

$$\boxed{\sum_i \rightarrow g \int \frac{d^3x d^3p}{(2\pi)^3}.} \quad (4.38)$$

Discrete quantum numbers, such as spin, isospin, and flavor, contribute an additive component of the same form in the sum over the single-particle states, which gives rise to the degeneracy coefficient g in Eq. (4.38). Aside from the volume term shown in Eq. (4.38), there is, in general, also a correction that has the form of a surface term. The magnitude and sign of the surface term depend on the physical problem considered. We will not pursue this topic further in this book; for a general discussion of this subject see, e.g., [51, 52].

4.4 The Fermi and Bose quantum gases

Allowing for the presence both of particles and of antiparticles, the quantum-statistical grand partition function Eq. (4.28) for a particle of mass m and degeneracy g can be written explicitly as

$$\boxed{\ln \mathcal{Z}_{F/B}(V, \beta, \lambda, \gamma) = \pm gV \int \frac{d^3p}{(2\pi)^3} \left[\ln(1 \pm \gamma \lambda e^{-\beta\sqrt{p^2+m^2}}) + \ln(1 \pm \gamma \lambda^{-1} e^{-\beta\sqrt{p^2+m^2}}) \right].} \quad (4.39)$$

The second term in Eq. (4.39) is due to antiparticles. The well-known ‘classical’ Boltzmann limit arises from expansion of the logarithms, i.e., when it is possible to consider the exponential term as small relative to unity:

$$\boxed{\ln \mathcal{Z}_{cl}(V, \beta, \lambda, \gamma) = gV \int \frac{d^3p}{(2\pi)^3} \gamma(\lambda + \lambda^{-1}) e^{-\beta\sqrt{p^2+m^2}}.} \quad (4.40)$$

We will often use the (normalized) particle *spectrum*, the average relative probability of finding a particle at the energy E_i , which is the coefficient of E_i in Eq. (4.13). Using Eqs. (4.8) and (4.10) we obtain

$$\begin{aligned} \overline{w}_i &\equiv \frac{\bar{n}_i}{N} = \frac{e^{-\beta E_i}}{\sum_j e^{-\beta E_j}} \\ &= -\frac{1}{\beta} \frac{\partial}{\partial E_i} \left(\ln \sum_j \gamma e^{-\beta E_j} \right) = -\frac{1}{\beta} \frac{\partial}{\partial E_i} \ln Z. \end{aligned} \quad (4.41)$$

The single-particle spectrum that follows from Eq. (4.28) is easily evaluated,

$$f_{\text{F/B}}(\varepsilon; \beta, \lambda, \gamma) = \frac{1}{\gamma^{-1} \lambda^{-1} e^{\beta \varepsilon} \pm 1}, \quad (4.42)$$

where the plus sign applies for fermions, and the minus sign for bosons. For antiparticles, we replace λ by λ^{-1} . The classical Boltzmann approximation arises again in the limit in which it is possible to neglect the term ± 1 in the denominator, i.e., when the phase-space abundance is small,

$$f_{\text{F/B}} \rightarrow f_{\text{cl}} = \gamma \lambda e^{-\beta \varepsilon}, \quad (4.43)$$

where $\lambda \rightarrow 1/\lambda$ for antiparticles. More generally, for $\gamma \lambda e^{-\beta \varepsilon} < 1$, this Stefan–Boltzmann spectral shape can be written as an infinite series:

$$f_{\text{F/B}} = \pm \sum_{n=1}^{\infty} \left(\pm \gamma \lambda e^{-\beta \varepsilon} \right)^n. \quad (4.44)$$

We consider, as an example, the spectra and yield of gluons, a special case of interest to us among bosons. Their behavior is similar to the case of photons ($g_\gamma = 2$) but gluons have an eight-fold greater color degeneracy ($g_g = 16$). Both photons and gluons do not have an antiparticle partner, and their number is unrestricted by particle/antiparticle conservation; hence $\lambda \rightarrow 1$. We obtain

$$\ln \mathcal{Z}_{\gamma, g} = -g_{\gamma, g} V \int \frac{d^3 p}{(2\pi)^3} \ln(1 - \gamma e^{-\beta \varepsilon}), \quad (4.45)$$

where $\varepsilon = \varepsilon(\vec{p}) = \sqrt{m^2 + \vec{p}^2} \rightarrow |\vec{p}|$, except when we consider a non-vanishing thermal gluon mass in the medium. The particle occupation probability is

$$f_{\gamma, g}(\varepsilon) = \frac{1}{\gamma^{-1} e^{\beta \varepsilon} - 1} = \sum_{n=1}^{\infty} \gamma^n e^{-n\beta \varepsilon}, \quad \gamma < e^{\beta m}. \quad (4.46)$$

The gluon (and photon) particle densities are

$$\rho_{\gamma,g} \equiv \frac{N_{\gamma,g}}{V} = \frac{1}{V} \lim_{\lambda \rightarrow 1} \lambda \frac{d}{d\lambda} \ln \mathcal{Z}_{\gamma,g} = g_{\gamma,g} \int \frac{d^3p}{(2\pi)^3} f_{\gamma,g}. \quad (4.47)$$

Using the series expansion from Eq. (4.46), we can explicitly evaluate this integral, substituting np/T for x term by term:

$$\rho_{\gamma,g} = \frac{g_{\gamma,g}}{2\pi^2} T^3 \sum_{n=1}^{\infty} \frac{\gamma^n}{n^3} \int_0^{\infty} dx x^2 e^{-\sqrt{(nm/T)^2 + x^2}}. \quad (4.48)$$

For $m \rightarrow 0$ and $\gamma \rightarrow 1$, we obtain the well-known Stefan–Boltzmann equilibrium limit:

$$\rho_{\gamma,g} = \frac{g_{\gamma,g}}{\pi^2} T^3 \zeta(3), \quad (4.49)$$

with the Riemann zeta-function $\zeta(3) \simeq 1.202$; see Eq. (10.66b). Using Eq. (10.50a), for the general case, to evaluate the integral, we obtain an infinite sum over terms containing the Bessel function K_2 (also called the McDonald function), which is discussed in section 10.4:

$$\rho_{\gamma,g} = \frac{g_{\gamma,g}}{\pi^2} T m^2 \sum_{n=1}^{\infty} \frac{\gamma^n}{n} K_2(nm/T). \quad (4.50)$$

Many other properties of the quark–gluon gas are discussed in section 10.5.

The statistical method is a powerful tool to deal with the physics we address in this book. Looking back, we recognize that we have assumed the presence of sufficiently many (weakly) interacting (quasi)particles in this discussion of basic results of statistical physics. Two important questions come to mind.

- In our context, the practical question is that of how statistical physics works when we have a few hundred (at the SPS), or a few thousand (at the RHIC) particles experiencing a limited number of collisions each. In this book, we will answer this question by consulting the experimental results, and our finding is that the thermal particle spectra describe experimental data very well.
- It seems that, perhaps, we could derive statistical-physics laws for any type of many-object system – could it be that the statistical partition function even describes the behavior of investors on Wall Street? Let us clearly identify what specific tacit physical feature makes a system of particles so much simpler to understand than a crowd of investors. An appropriate economical toy model, in our context, would consist of taking a ‘conserved’ number of Wall Street investors who, in view of their frequent interactions, should see their investments equipartitioned

into an exponential wealth distribution, provided that all members of the same wealth class are, basically, indistinguishable, a hypothesis many of our colleagues agree with. All the above equations apply, with E_i being now the wealth range of n_i investors. To compute anything with precision we need, however, to specify the meaning of the discrete sum, \sum_i ; we need to know the number of ‘investors’ per unit of ‘wealth’. In case of physical particles, this level density Eq. (4.37) is implicit in our understanding of the many particle *phase space*, which allows us to convert the symbolic expressions into quantitative equations. We are not able to generalize this naively to non-physics applications of statistical physics.

4.5 Hadron gas

Particularly important in our study is the hadronic ‘gas’ (HG) matter consisting of individually confined hadronic particles. Although relativistic dynamics is required, we can consider the classical (Boltzmann)-gas limit Eq. (4.40) since, in a very ‘rich’ multicomponent phase, each particle species has a rather low ‘non-degenerate’ phase-space abundance. In other words, at sufficiently high temperature, a high density of hadronic particles can arise as a consequence of many hadron species contributing, and does not in general imply a quantum degeneracy of the phase space. However, even in the HG phase, it is possible to encounter (pion) quantum degeneracy, which requires full quantum statistics, Eq. (4.39).

To see why the classical Boltzmann distribution almost always suffices in the hadronic gas phase of matter, consider the denominator of the quantum distribution, Eq. (4.42): even for the least-massive hadronic particle, the pion, the expansion of the denominator of quantum distributions makes good sense. For a range of temperatures up to $T < 150$ MeV wherein confined hadrons exist, we find $\exp(-E_\pi/T) < \exp(-m_\pi/T) < 1$. The limits of the Boltzmann approximation are tested when, e.g., the phase space is oversaturated, i.e., $\gamma_\pi > 1$, or when the baryo-chemical potential compensates for the mass term which could occur in extremely dense baryonic systems.

We present next a brief survey of the properties of a hadronic Boltzmann gas, and refer to chapter 10 for further developments. We consider a series expansion of the logarithmic function in Eq. (4.39):

$$\ln \mathcal{Z} = \sum_{n=1}^{\infty} \frac{1}{n} Z_n. \quad (4.51)$$

Each term comprises contributions from all contributing bosons B_f and

fermions F_f :

$$Z_n = \sum_{B_f} g_f \gamma_f^n (\lambda_f^n + \lambda_f^{-n}) V \int \frac{d^3p}{(2\pi)^3} e^{-n\beta\varepsilon_f} + (-)^{n+1} \sum_{F_f} g_f \gamma_f^n (\lambda_f^n + \lambda_f^{-n}) V \int \frac{d^3p}{(2\pi)^3} e^{-n\beta\varepsilon_f}. \quad (4.52)$$

The single-particle energy ε_f entering Eq. (4.52) depends on the mass m_f of particle f , Eq. (4.31). Since the mass spectra of hadronic bosons and fermions are quite different, $n > 1$ quantum corrections do not cancel out.

In the Boltzmann limit, the first term $n = 1$ is retained in Eq. (4.51) and there is no distinction between the Bose and Fermi ideal gases in this ‘classical’ limit, as seen in Eq. (4.40):

$$\ln Z_{cl} = \sum_f g_f \gamma (\lambda_f + \lambda_f^{-1}) V \int \frac{d^3p}{(2\pi)^3} e^{-\beta\varepsilon(\vec{p})} \equiv Z^{(1)}. \quad (4.53)$$

The last definition reminds us that the right-hand side of Eq. (4.53) is the partition function arising for a single particle enclosed in a given volume. This is not an entirely ‘classical’ expression. We note that

$$Z_{cl} = \sum_{k=0}^{\infty} \frac{1}{k!} (Z^{(1)})^k, \quad (4.54)$$

which expresses the fact that the partition function comprises the additive contributions of terms for k microscopic particles. However, the quantum indistinguishability is retained in the factor $1/k!$ – only with this quantum factor can one obtain the correct ‘classical’ Maxwell distribution of atoms in a gas. This issue marked strongly the pre-quantum-mechanics development of statistical physics in the Boltzmann era since there was no easy explanation why this factor was needed.

We already know the momentum integral appearing in Eq. (4.53), from Eq. (4.48),

$$\ln Z_{cl} = \frac{\beta^{-3}V}{2\pi^2} \sum_f g_f \gamma (\lambda_f + \lambda_f^{-1}) W(\beta m_f), \quad (4.55)$$

where we used the function $W(x) = x^2 K_2(x)$, shown in Fig.10.1 on page 197.

Using Eq. (4.55), we obtain the properties of a hadronic gas in the classical (Boltzmann) limit. The ‘net’ (particle minus antiparticle) particle density, Eq. (4.22),

$$\rho_f = \frac{T^3}{2\pi^2} \sum_f g_f \gamma (\lambda_f - \lambda_f^{-1}) (\beta m_f)^2 K_2(\beta m_f), \quad (4.56)$$

pressure,

$$P_{cl} = \frac{T}{V} \ln \mathcal{Z}_{cl} = \frac{T^4}{2\pi^2} \sum_f g_f \gamma_f (\lambda_f + \lambda_f^{-1}) (\beta m_f)^2 K_2(\beta m_f), \quad (4.57)$$

and energy density,

$$\begin{aligned} \epsilon_{cl} = -\frac{1}{V} \frac{\partial}{\partial \beta} \ln \mathcal{Z}_{cl} &= \frac{T^4}{2\pi^2} \sum_f g_f \gamma_f (\lambda_f + \lambda_f^{-1}) \\ &\times [3(\beta m_f)^2 K_2(\beta m_f) + (\beta m_f)^3 K_1(\beta m_f)]. \end{aligned} \quad (4.58)$$

comprise the sum over all particle fractions. In Eq. (4.56) we obtained the difference between numbers of particles and antiparticles. The relation between partition function and pressure which we introduced in Eq. (4.57) is discussed in section 10.1, see Eq. (10.11). To obtain Eq. (4.58), we used $dx^2 K_2(x)/dx = -x^2 K_1(x)$.

The relativistic limits of Eqs. (4.57) and (4.58) arise in view of the properties of the Bessel function, Eqs. (10.47) and (10.50b), $K_2(x) \rightarrow 2/x^2$ and $K_1(x) \rightarrow 1/x$, and only the K_2 term contributes:

$$\begin{aligned} P_{cl} &\rightarrow \frac{T^4}{\pi^2} \sum_f g_f \gamma_f (\lambda_f + \lambda_f^{-1}), \\ \epsilon_{cl} &\rightarrow \frac{3T^4}{\pi^2} \sum_f g_f \gamma_f (\lambda_f + \lambda_f^{-1}). \end{aligned} \quad (4.59)$$

In the case of fermions, the Pauli exclusion principle decreases the particle degeneracy below the classical value. The energy and pressure shown in Eq. (4.59) are reduced in the relativistic limit by the Riemann η -function factor $\eta(4) = \frac{7}{8}\pi^4/90 = 0.9470$. On the other hand, since bosons are ‘attracted’ to each other, one finds a greater than classical degeneracy, expressed in the relativistic limit by the factor $\zeta(4) = \pi^4/90 = 1.0823$.

For a relativistic hadron gas, comprising a similar number of fermions and bosons, this quantum effect averages out. Thus, when we speak of an effective number of degrees of freedom (also effective degeneracy) in HG, we will use as a basis the classical expression Eq. (4.59):

$$g_{\text{eff}}^P \equiv \pi^2 \frac{P}{T^4}, \quad g_{\text{eff}}^\epsilon \equiv \frac{\pi^2}{3} \frac{\epsilon}{T^4}. \quad (4.60)$$

When $T \gg m$ for all particles, or, equivalently, when T is the only relevant energy scale, we have $g_{\text{eff}}^P \simeq g_{\text{eff}}^\epsilon$.

We consider, in Fig. 4.1, how g_{eff}^P and g_{eff}^ϵ look in a simple hadronic gas, as functions of T . Solid lines correspond to g_{eff}^ϵ , and dashed to g_{eff}^P . The thin lines are for the classical Boltzmann pion gas ($g_\pi = 3$, $m_\pi \simeq 140$

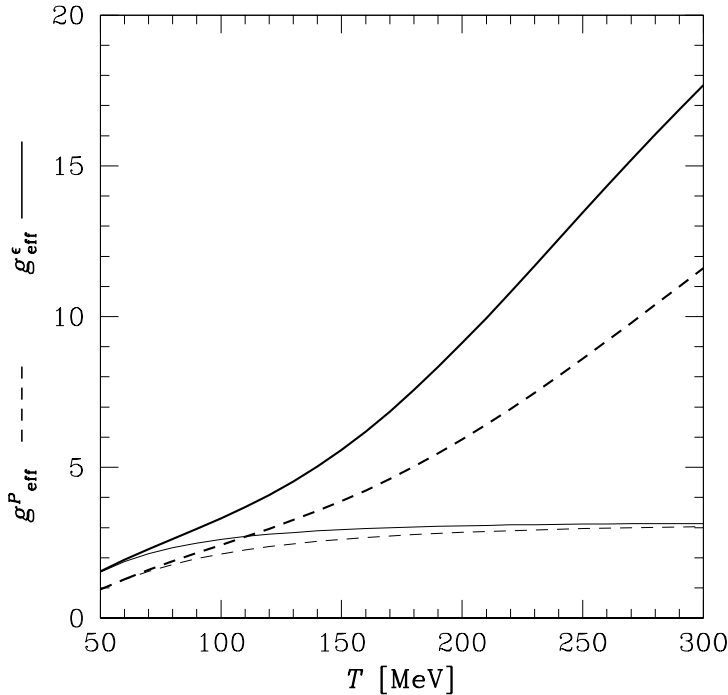


Fig. 4.1. Effective numbers of degrees of freedom from energy density (solid lines) and pressure (dashed lines), Eq. (4.60), for a Boltzmann pion gas (thin lines), and gas comprising Boltzmann pions, nucleons, kaons, and $\Delta(1232)$ for $\gamma_i = 1$ and $\lambda_i = 1$, as functions of temperature T .

MeV); thick lines also include the four kaons K , the nucleons N , and the deltas $\Delta(1232)$, and for N and Δ their antiparticles ($g_K = 4$, $m_K \simeq 495$ MeV; $g_N = 4$, $m_N \simeq 939$ MeV; and $g_\Delta = 16$, $m_\Delta \simeq 1232$ MeV) evaluated with all $\gamma = 1$, as appropriate for chemical equilibrium, and $\lambda = 1$, for a nearly baryon-free system, as appropriate for the early Universe. We see for the pion-only case (thin lines) the expected high- T limit, which is nearly reached already at $T \simeq m_\pi$. However, because of the relatively high hadron masses, the effective number of degrees of freedom keeps rising even at $T \simeq 300$ MeV toward its maximum for this example, which is near 50. We also note that the energy density approaches its relativistic limit faster than does the pressure, a point to which we shall return in Eq. (10.58).

We draw two important conclusion from results seen in Fig. 4.1.

- Since pions are several times lighter than the next heavier hadronic particle, they determine rather exactly the properties of a hadron gas at ‘low’ temperature below $T \simeq (m_\pi/2)$ MeV, as is seen in Fig. 4.1

(the case that the net baryon and strangeness density is zero). Even at $T \simeq m_\pi$, the pion fractional pressure is still the dominant component.

- The influence of the numerous massive hadronic particles rapidly gains in importance with rising temperature. At low temperature, the quantum corrections (not shown in Fig. 4.1) are in fact more important than the contributions of heavier particles since $2m_\pi < m_h, h \neq \pi$. For $2\beta m_\pi < 1$ in the HG phase, with $g_\pi = 3$, (for derivation compare Eq. (10.62)), we have

$$P_h^\pi \simeq \frac{3T^4}{2\pi^2} \left(\gamma_\pi \lambda_\pi W(\beta m_\pi) + \frac{1}{16} \gamma_\pi^2 \lambda_\pi^2 W(2\beta m_\pi) + \dots \right). \tag{4.61}$$

As the temperature increases, the small quantum correction remains a minor effect compared with a rise due to excitation of numerous heavy hadron states.

4.6 A first look at quark–gluon plasma

We consider next the properties of the QGP, modeled initially as an ideal chemically equilibrated gas of quarks and gluons, including the effect of confining vacuum structure. In the study of the quark-and-gluon gas, our task is considerably simplified by the observation that the gluons and light u and d quarks are to all intent massless particles, at least on the scale of energies available in the hot plasma, i.e., $T \approx 200$ MeV.

Since the energy density is, in general terms, given by (see Eqs. (10.7) and (10.11))

$$\epsilon = -\frac{\partial}{\partial \beta} \frac{1}{V} \ln \mathcal{Z}(\beta, \lambda), \tag{4.62}$$

in the absence of any dimensioned scales,

$$\frac{1}{V} \ln \mathcal{Z}(\beta, \lambda) = \beta^{-3} f(\lambda), \tag{4.63}$$

and we find

$$\epsilon = 3\beta^{-4} f(\lambda) = 3 \frac{T}{V} \ln \mathcal{Z}(\beta, \lambda) = 3P. \tag{4.64}$$

The presence of masses of quarks, and in general scaled variables, breaks this perhaps most used relationship of relativistic gases. It applies to fermions, bosons, and classical gases. Equations (10.58)–(10.60) show how the presence of masses reduces the pressure below $\epsilon/3$. Put differently, massive particles are less mobile at a given temperature, and thus the pressure they can exercise is smaller than $\epsilon/3$; the energy density ϵ is ‘helped’ by the presence of masses, and is closer to the relativistic limit.

In the limit $\beta m = m/T \ll 1$, the phase-space integrals of ideal quantum gases are easily carried out. We can effectively neglect the particle mass m compared with the high momenta that occur. We also omit, at first, chemical potentials. We obtain for the energy density

$$\frac{E_{F,B}}{V} = \frac{g}{2\pi^2} \int_0^\infty p^2 dp \frac{p}{e^{\beta p} \pm 1} = \frac{g\beta^{-4}}{2\pi^2} 3! \sum_1^\infty \frac{(\pm 1)^{n-1}}{n^4}. \tag{4.65}$$

The infinite sums are the zeta and eta Riemann sums, see Eqs. (10.66a)–(10.67b), which for bosons give the well-known Stefan–Boltzmann result:

$$\boxed{P_B|_{m=0} = \frac{T}{V} \ln \mathcal{Z}_B|_{m=0} = \frac{g\pi^2}{90} T^4 = \frac{1}{3} \epsilon_B \equiv \frac{E_B}{3V}.} \tag{4.66}$$

We have made explicit the result $\epsilon = 3P$, see Eq. (4.64), which is valid when the mass of particles is small relative to their energy (massless particles or ultra-relativistic gas). For fermions, the alternating sum in Eq. (4.65) introduces a relative reduction factor, which is $\frac{7}{8}$, see Eq. (10.67b). However, allowing for the presence of antifermions, the energy density and pressure have to be multiplied by an extra factor of two, and become in fact greater by a factor $\frac{7}{4}$:

$$\epsilon_F \equiv \frac{E_F}{V} = \frac{g\pi^2}{30} \frac{7}{4} T^4 = 3P_F. \tag{4.67}$$

For fermions, the inclusion of a finite chemical potential is of importance. In the limit $m \rightarrow 0$, the Fermi integrals of the relativistic quantum (degenerate) quark gas can be evaluated exactly at finite μ , see Eq. (10.73):

$$\boxed{P_F|_{m=0} = \frac{T}{V} \ln \mathcal{Z}_F|_{m=0} = g \frac{(\pi T)^4}{90\pi^2} \left(\frac{7}{4} + \frac{15\mu^2}{2(\pi T)^2} + \frac{15\mu^4}{4(\pi T)^4} \right).} \tag{4.68}$$

Since in the domain of freely mobile quarks and gluons the vacuum is deconfined, a finite vacuum energy density (the latent heat of the vacuum) arises within the deconfined region, as we have discussed at length in section 3.1. This also implies that there must be a (negative) associated pressure acting on the surface of this volume and attempting to reduce the size of the deconfined region. These two properties of the vacuum follow consistently from the vacuum partition function:

$$\boxed{\ln \mathcal{Z}_{\text{vac}} \equiv -\mathcal{B}V\beta.} \tag{4.69}$$

On differentiating Eq. (4.69) as in Eqs. (4.57) and (4.58), we in fact find that the perturbative vacuum region is subject to the (external) pressure $-\mathcal{B}$ while the internal energy density is $+\mathcal{B}$ relative to the outside volume.

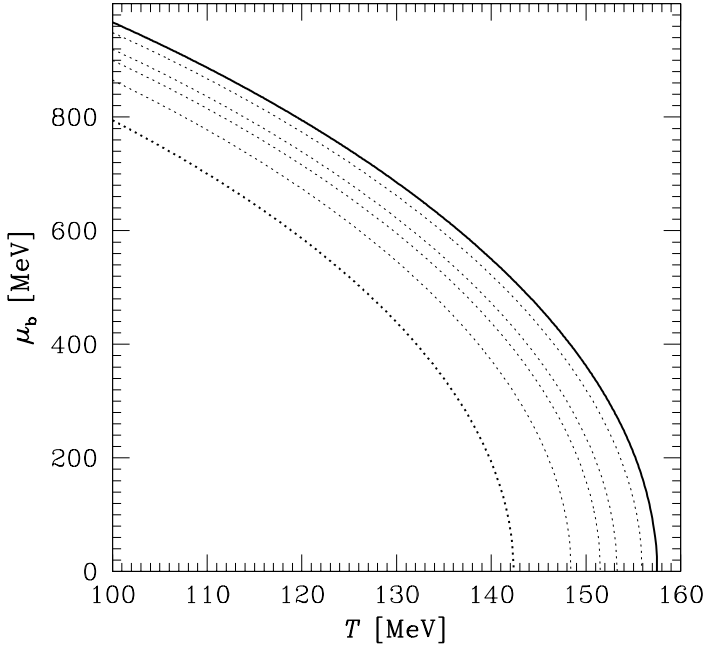


Fig. 4.2. $P = 0$ in the quark–gluon liquid in the (μ_b-T_c) plane. Dotted (from right to left): breakup conditions of the liquid for expansion velocities $v^2 = \frac{1}{10}, \frac{1}{6}, \frac{1}{5}, \frac{1}{4}$ and $\frac{1}{3}$.

The partition function (i.e., pressure) of the quark–gluon phase is obtained after we combine contributions from quarks, gluons, and vacuum:

$$\boxed{\frac{T}{V} \ln \mathcal{Z}_{\text{QGP}} \equiv P_{\text{QGP}} = -\mathcal{B} + \frac{8}{45\pi^2} c_1 (\pi T)^4 + \frac{n_f}{15\pi^2} \left[\frac{7}{4} c_2 (\pi T)^4 + \frac{15}{2} c_3 \left(\mu_q^2 (\pi T)^2 + \frac{1}{2} \mu_q^4 \right) \right]} \quad (4.70)$$

We have inserted the quark and gluon degeneracies as shown in Eqs. (3.35a) and (3.35b). The interactions between quarks and gluons manifest their presence aside from the vacuum-structure effect, in the three coefficients $c_i \neq 1$, see Eqs. (16.1) and (16.2), [91]:

$$c_1 = 1 - \frac{15\alpha_s}{4\pi} + \dots, \quad (4.71a)$$

$$c_2 = 1 - \frac{50\alpha_s}{21\pi} + \dots, \quad (4.71b)$$

$$c_3 = 1 - \frac{2\alpha_s}{\pi} + \dots. \quad (4.71c)$$

One can evaluate the pressure Eq. (4.70) by choosing values for \mathcal{B} and α_s . It turns out that the value of the running strong-interaction coupling constant α_s changes rather rapidly in the domain of interest to us, and hence one needs to employ a function $\alpha_s(T)$, see Fig. 14.3 on page 286. Then, also allowing for the latent heat \mathcal{B} , a surprisingly good agreement with lattice results in section 15.5 is found, this is shown in Fig. 16.2 on page 307. This comparison hinges strongly on an understanding of $\alpha_s(T)$, and inclusion of \mathcal{B} .

Drawing on these considerations, we show the QGP-phase pressure condition $P_{\text{QGP}} \rightarrow 0$ in Fig. 4.2. The solid line denotes, in the $(\mu_b - T_c)$ plane, where $P_{\text{QGP}} = 0$ in a stationary quark-gluon phase. The dotted lines correspond (from right to left) to the condition Eq. (3.31) for flow velocities $v^2 = \frac{1}{10}, \frac{1}{6}, \frac{1}{5}, \frac{1}{4}$ and $\frac{1}{3}$ for which an exact spherical expansion with $\kappa = 1$, see Eq. (3.32), was used. The last dotted line to the left corresponds to an expansion with the velocity of sound of relativistic (i.e., effectively massless) matter. For small baryo-chemical potentials, the equilibrium phase-transition temperature of a non-dynamically evolving system is somewhat greater than that shown here at the intercept of the solid line at $\mu_b = 0$. The actual value is $T_c \simeq 170$ MeV, as it occurs at finite pressure balanced by hadrons, compare with Fig. 3.2. Looking at the high-flow-velocity curves in Fig. 4.2, we see that an exploding QGP fireball can supercool to $T \simeq 0.9T_c$.